

# Quantum Monte Carlo simulation of three-dimensional Bose-Fermi mixtures

Arata Yamamoto<sup>1</sup> and Tetsuo Hatsuda<sup>1,2</sup>

<sup>1</sup>*Theoretical Research Division, Nishina Center, RIKEN, Saitama 351-0198, Japan*

<sup>2</sup>*IPMU, The University of Tokyo, Kashiwa 277-8583, Japan*

(Dated: October 21, 2018)

Exploratory simulations of Bose-Fermi mixtures on the three-dimensional optical lattice at finite temperature are performed by adopting the lattice quantum chromodynamics technique. We analyze the bosonic superfluid transition and its dependence on the strength of the boson-fermion coupling. The particle densities and the pair occupancies are also studied to understand the effect of the boson-fermion coupling to the microscopic properties of the system. Effect of the induced fermion-fermion interaction by the boson density fluctuation is clearly seen.

PACS numbers: 03.75.Lm, 03.75.Mn, 37.10.Jk, 71.10.Fd

## I. INTRODUCTION

Many-body mixture of bosons and fermions is an interesting quantum system. It is not only useful to study the interplay between different quantum statistics in condensed matter physics and in atomic physics [1], but also important for understanding the hadron-quark phase transition in nuclear and particle physics [2]. Recently, many kinds of Bose-Fermi mixtures have been realized in ultracold atomic experiments. In particular, the Bose-Fermi mixtures such as <sup>87</sup>Rb-<sup>40</sup>K [3–5], <sup>170</sup>Yb-<sup>173</sup>Yb and <sup>174</sup>Yb-<sup>173</sup>Yb [6] can be trapped in three-dimensional optical lattices.

Despite of its importance, ab initio quantum Monte Carlo calculations of the Bose-Fermi Hubbard model, which is a model system of the Bose-Fermi mixture on the optical lattice, have been limited to one spatial dimension [7–13]. (See also a recent review [14].) These simulations were done with improved versions of the world-line formalism [15–17]. The world-line formalism is an exact scheme in one spatial dimension while it has the fermion sign problem in higher dimensions.

In this paper, we apply the method of lattice Monte Carlo simulation of quantum chromodynamics (QCD) [18] to overcome the fermion sign problem in the Bose-Fermi mixture of ultracold atoms on an optical lattice in three spatial dimensions at finite temperature. The lattice QCD simulation is an established numerical framework for the strongly coupled regime of QCD; the mixture of gluons (bosons) and quarks (fermions) can be treated in any dimension without fermion sign problem as long as the fermion determinant is real and semi-positive. (For relativistic fermions with finite chemical potential, the fermion determinant becomes complex, while the

chemical potential for non-relativistic fermions does not cause the problem.)

This paper is organized as follows. In Sec. II, we introduce the model action and discuss the basic setup of our simulations. In Sec. III, we analyze the bosonic superfluid transition and its dependence on the strength of the boson-fermion coupling. The particle densities and the pair occupancies are also studied to understand the effect of the boson-fermion coupling. In Sec. IV, we summarize this study. A part of the preliminary results was reported in Ref. [19].

## II. FORMULATION

We consider one-component boson field  $\Phi(\vec{x}, \tau)$  and two-component fermion field  $\Psi_\uparrow(\vec{x}, \tau)$  and  $\Psi_\downarrow(\vec{x}, \tau)$ . The partition function  $Z$  is then written as a path integral in terms of the Euclidean action  $S$ :

$$\begin{aligned} Z &= \int D\Phi^* D\Phi D\Psi_\uparrow^* D\Psi_\uparrow D\Psi_\downarrow^* D\Psi_\downarrow e^{-S} \\ &= \int D\Phi^* D\Phi \det K_\uparrow \det K_\downarrow e^{-S_B}. \end{aligned} \quad (1)$$

In the second line, the bilinear form of the fermion fields are integrated out, so that  $Z$  becomes a functional only of the boson field.

We adopt the single-band Bose-Fermi Hubbard model whose lattice action reads [19–21]

$$S = S_B + S_F + S_{BF}, \quad (2)$$

$$\begin{aligned} S_B &= \sum_{\vec{x}, \tau} \left[ \Phi^*(\vec{x}, \tau) \{ \Phi(\vec{x}, \tau) - e^{\mu_B} \Phi(\vec{x}, \tau - 1) \} - \sum_{j=1}^3 t_B \{ \Phi^*(\vec{x}, \tau) \Phi(\vec{x} + \vec{e}_j, \tau) + \Phi^*(\vec{x}, \tau) \Phi(\vec{x} - \vec{e}_j, \tau) \} \right. \\ &\quad \left. + U_{BB} \Phi^*(\vec{x}, \tau) \Phi(\vec{x}, \tau) \{ \Phi^*(\vec{x}, \tau) \Phi(\vec{x}, \tau) - 1 \} \right] \end{aligned} \quad (3)$$

$$S_F = \sum_{\vec{x}, \tau, \sigma} \left[ \Psi_\sigma^*(\vec{x}, \tau) \{ \Psi_\sigma(\vec{x}, \tau) - e^{\mu_F} \Psi_\sigma(\vec{x}, \tau - 1) \} - \sum_{j=1}^3 t_F \{ \Psi_\sigma^*(\vec{x}, \tau) \Psi_\sigma(\vec{x} + \vec{e}_j, \tau) + \Psi_\sigma^*(\vec{x}, \tau) \Psi_\sigma(\vec{x} - \vec{e}_j, \tau) \} \right] \quad (4)$$

$$S_{BF} = \sum_{\vec{x}, \tau, \sigma} U_{BF} \Phi^*(\vec{x}, \tau) \Phi(\vec{x}, \tau) \Psi_\sigma^*(\vec{x}, \tau) \Psi_\sigma(\vec{x}, \tau - 1). \quad (5)$$

Here,  $\mu_B$  ( $\mu_F$ ) is the boson (fermion) chemical potential,  $t_B$  ( $t_F$ ) is the spatial hopping parameters for the boson (fermion). Also,  $U_{BB}$  and  $U_{BF}$  are the strength of boson-boson interaction and boson-fermion interaction, respectively. We do not consider the fermion-fermion interaction for simplicity, i.e.  $U_{FF} = 0$ . The temporal hopping structures of the chemical potential and the interaction are based on Refs. [20, 21].

Note that we have absorbed the spatial lattice spacing  $a_s$  and the temporal lattice spacing  $a_\tau$  into the definition of the fields and the coupling parameters. Here  $a_s$  should be identified with a finite lattice constant of an optical lattice, while  $a_\tau$  should be eventually taken to be zero to recover the continuum limit in the temporal direction. In the following discussion, all dimensional quantities are scaled by the lattice constant.

Our lattice action has the boson sign problem which appears in non-relativistic systems. The boson action is complex in general because the temporal hopping term is given as  $\sum_\tau \Phi^*(\vec{x}, \tau) \{ \Phi(\vec{x}, \tau) - \Phi(\vec{x}, \tau - 1) \} = N_\tau \sum_\nu \{ 1 - e^{-i\omega_B(\nu)} \} \tilde{\Phi}^*(\vec{x}, \nu) \tilde{\Phi}(\vec{x}, \nu)$  with the boson Matsubara frequency  $\omega_B(\nu) = 2\nu\pi T$ . To avoid this boson sign problem, we adopted the zero-frequency approximation, in which the boson field is projected onto the zero-frequency mode as  $\Phi(\vec{x}, \tau) = \tilde{\Phi}(\vec{x}, \nu = 0) \equiv \Phi(\vec{x})$ . This approximation is validated if the system is either in the critical region or in the high-temperature limit, where the static mode of the boson field,  $\nu = 0$ , gives a dominant contribution. Furthermore, effect of the non-zero Matsubara modes can be estimated by using the reweighting method [22].

We can prove that the fermion determinant is real and positive. Let us consider the fermion action in the frequency space. The matrix  $K_\sigma$  becomes diagonal in the frequency space. The complex factor is only  $e^{-i\omega_F(\nu)}$  with the fermion Matsubara frequency  $\omega_F(\nu) = (2\nu - 1)\pi T$ . The fermion determinant is

$$\begin{aligned} \det K_\sigma &= \prod_\nu (A + e^{-i\omega_F(\nu)} B) \\ &= \prod_{\omega_F(\nu) > 0} [\{A + B \cos \omega_F(\nu)\}^2 + B^2 \sin^2 \omega_F(\nu)] \\ &> 0, \end{aligned} \quad (6)$$

where  $A$  and  $B$  are real numbers. Therefore, there arises no sign problem originating from the fermion determinant. (This is in contrast to the Bose-Fermi system with a Yukawa coupling discussed e.g. in Ref. [23].) Even if the fermion-fermion interaction is introduced, there is no fermion sign problem: After the Hubbard-Stratonovich

transformation of the fermion-fermion interaction,  $K_\sigma$  is still a real matrix with auxiliary fields, so that the two-component fermion determinant becomes semi-positive,  $\det K_\uparrow \det K_\downarrow = (\det K_\uparrow)^2 \geq 0$ .

Our numerical simulation procedure is based on the hybrid Monte Carlo algorithm with the pseudofermions [24], which is widely used in modern simulations of lattice field theories. For preconditioning the fermion matrix, we perform a Fourier transformation from the imaginary time  $\tau$  to the fermion Matsubara frequency  $\omega_F(\nu)$ . In this study, we fixed the hopping parameters  $t_B = t_F = 0.01$  and the repulsive boson-boson interaction  $U_{BB} = 0.1$  for the first trial. We performed the simulation in a spatial lattice volume  $V = N_s^3 = 10^3$  with periodic boundary conditions. We varied temperature  $T = 1/N_\tau$  by changing the temporal lattice size as  $N_\tau = 20, 30, 40, 60$ , and 100.

In the grand-canonical approach, particle number densities are related to chemical potentials and other parameters. Therefore, we monitor the boson number density  $n_B$  and fermion number density  $n_F$  in our simulations:

$$n_B = \langle \Phi^*(\vec{x}) \Phi(\vec{x}) \rangle, \quad (7)$$

$$n_F = \langle \Psi_\uparrow^*(\vec{x}, \tau) \Psi_\uparrow(\vec{x}, \tau) \rangle = \langle \Psi_\downarrow^*(\vec{x}, \tau) \Psi_\downarrow(\vec{x}, \tau) \rangle. \quad (8)$$

Note that, in the mean-field level, the boson-fermion coupling  $U_{BF}$  induces effective chemical potentials:

$$\mu_B^{\text{eff}} \sim \mu_B - U_{BF} n_F, \quad (9)$$

$$\mu_F^{\text{eff}} \sim \mu_F - U_{BF} n_B. \quad (10)$$

This implies that attractive boson-fermion interaction ( $U_{BF} < 0$ ) increases the effective chemical potentials and hence the particle number densities. Our numerical simulations given below indeed show such behavior.

### III. NUMERICAL RESULTS

To see the effect of  $U_{BF}$  on the Bose-Einstein condensation, let us first examine the boson propagator as a function of the distance  $r = |\vec{x} - \vec{y}|$ ,

$$G_B(r) = \langle \Phi^*(\vec{x}) \Phi(\vec{y}) \rangle. \quad (11)$$

The boson propagator  $G_B(r)$  with  $U_{BF} = 0$  and  $\mu_F = \mu_B = 0$  is shown in Fig. 1. Although the statistical errors are shown by the error-bars in the figure, they are smaller than the size of the symbols and practically invisible. At high temperature ( $T > 0.02$ ),  $G_B(r)$  drops to zero exponentially, while at low temperature ( $T < 0.02$ ),

$G_B(r)$  approaches to a constant value for large  $r$ , i.e. a signature of the off-diagonal long-range order.

In Fig. 2, we draw the boson condensate fraction defined by

$$R_B = \frac{G_B(r = N_s/2)}{G_B(r = 0)}, \quad (12)$$

for different values of  $T$  and  $U_{BF}$  at  $\mu_F = \mu_B = 0$ . The blue region corresponds to the superfluid phase. The figure shows that the superfluid region is enlarged as the boson-fermion attraction ( $U_{BF} < 0$ ) becomes strong. This is because  $\mu_B^{\text{eff}}$  and hence the boson number density  $n_B$  increase associated with the increase of the boson-fermion attraction.

To see the effect of  $U_{BF}$  on particle number profiles in more details, let us introduce normalized pair occupancies which is a measure to find a pair at the same lattice

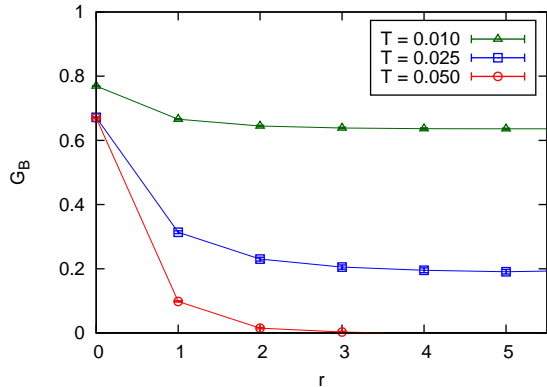


FIG. 1: The boson propagator  $G_B(r)$  as a function of  $r = |\vec{x} - \vec{y}|$  for different values of temperature  $T$  with  $U_{BF} = 0$  and  $\mu_F = \mu_B = 0$ .

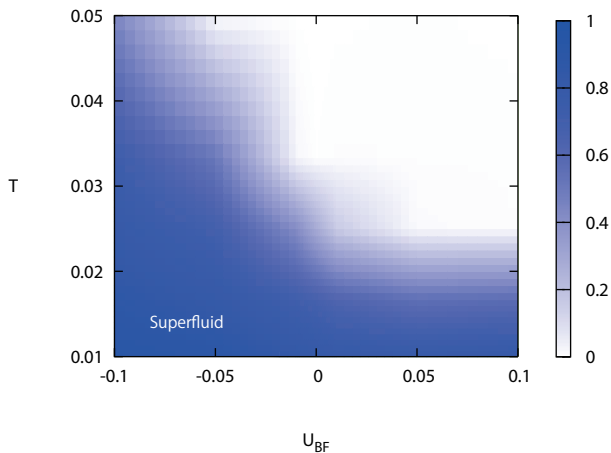


FIG. 2: The bosonic condensate fraction  $R_B$  in the  $T$ - $U_{BF}$  plane at  $\mu_F = \mu_B = 0$ .

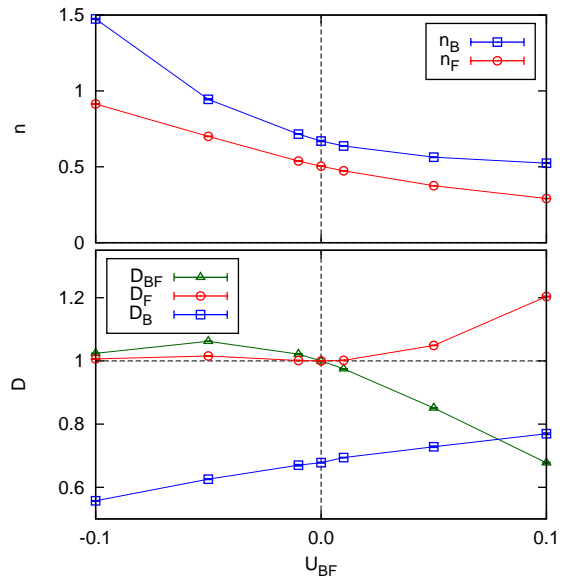


FIG. 3: The particle number densities and pair occupancies at  $\mu_B = \mu_F = 0$  and  $T = 0.05$  as a function of  $U_{BF}$ .

site;

$$D_{BF} = \frac{\langle n_B(\vec{x})n_{F\sigma}(\vec{x}) \rangle}{\langle n_B(\vec{x}) \rangle \langle n_{F\sigma}(\vec{x}) \rangle} \quad (13)$$

$$D_F = \frac{\langle n_{F\uparrow}(\vec{x})n_{F\downarrow}(\vec{x}) \rangle}{\langle n_{F\uparrow}(\vec{x}) \rangle \langle n_{F\downarrow}(\vec{x}) \rangle} \quad (14)$$

$$D_B = \frac{1}{2} \frac{\langle n_B(\vec{x})n_B(\vec{x}) \rangle}{\langle n_B(\vec{x}) \rangle^2}. \quad (15)$$

Here the number density operators are defined as  $n_B(\vec{x}) \equiv \Phi^*(\vec{x})\Phi(\vec{x})$  and  $n_{F\sigma}(\vec{x}) \equiv \Psi_\sigma^*(\vec{x}, \tau)\Psi_\sigma(\vec{x}, \tau)$ . The coefficient  $1/2$  in  $D_B$  is a symmetry factor for identical particles. The pair occupancies are experimentally observed on a three-dimensional optical lattice [6].

In Fig. 3, we show the particle number densities ( $n_B$  and  $n_F$ ) and the pair occupancies ( $D_{BF}$ ,  $D_F$ , and  $D_B$ ) as a function of  $U_{BF}$ . The chemical potentials are fixed at  $\mu_B = \mu_F = 0$  as in the previous figures, while the temperature is chosen to be  $T = 0.05$  (upper boundary in Fig. 2). As the boson-fermion attraction becomes stronger, both  $n_B$  and  $n_F$  increase, which is consistent with the behavior expected from the effective chemical potentials as we have already mentioned. Also, the pair occupancy of different (same) species tends to be enhanced (suppressed) as  $U_{BF}$  increases, which is naturally expected from the contact nature of the boson-fermion interaction. Note that  $D_B$  is always below unity, since we have taken repulsive boson-boson interaction.

In Figs. 4 and 5, we show the particle profiles as a function of the fermion chemical potential  $\mu_F$  for characteristic boson-fermion interactions; an attractive case,  $U_{BF} = -0.05$ , and a repulsive case,  $U_{BF} = +0.05$ . Other parameters are the same as those adopted in Fig. 3. By

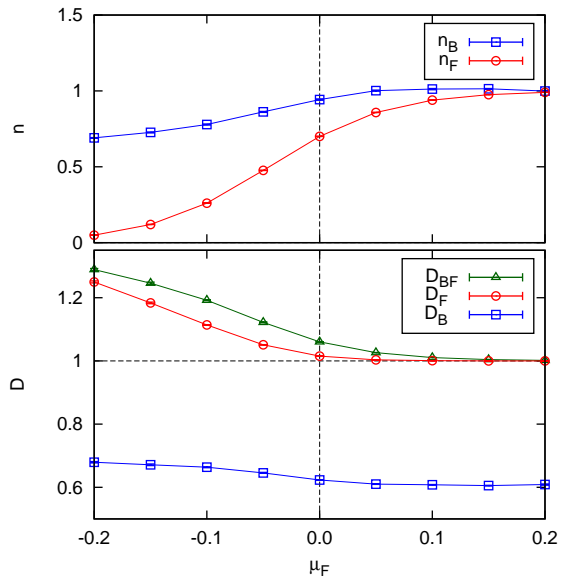


FIG. 4: The particle profiles as a function of  $\mu_F$  for attractive boson-fermion interaction  $U_{BF} = -0.05$ . Other parameters are the same with Fig. 3.

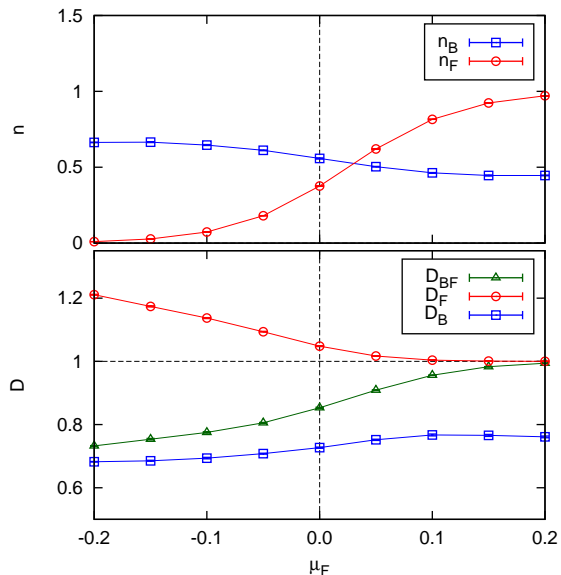


FIG. 5: The particle profiles as a function of  $\mu_F$  for repulsive boson-fermion interaction  $U_{BF} = +0.05$ . Other parameters are the same with Fig. 3.

varying  $\mu_F$  in the interval  $[-0.2, +0.2]$ , the fermion number density  $n_F$  is changed from zero (i.e. complete vacancy) to unity (i.e. full occupancy). The boson number density  $n_B$  is an increasing (decreasing) function of  $\mu_F$  in the attractive (repulsive) case, which is consistent with the behavior expected from the effective chemical potential  $\mu_B^{\text{eff}}$  in Eq. (9). Also, the boson-fermion

pair occupancy  $D_{BF}$  is reduced (enhanced) from unity in the repulsive (attractive) case as naturally expected from the contact nature of the boson-fermion interaction. The fermion number density approaches to unity, when  $\mu_F^{\text{eff}}$  in Eq. (10) becomes large either by large attractive boson-fermion interaction or by large fermion chemical potential. If fermions fully occupy all the lattice sites, both  $D_{BF}$  and  $D_F$  become unity, since the numerators of Eqs. (13) and (14) factorize.

Although the bare fermion-fermion interaction is switched off in our present simulations ( $U_{FF} = 0$ ), there arises induced fermion-fermion attraction due to the coupling of the fermions to the boson density fluctuation with the magnitude of  $O(U_{BF}^2/U_{BB})$  [1]. Because of this, the fermion pair occupancy  $D_F$  is enhanced irrespective of the sign of  $U_{BF}$  as seen in Figs. 4 and 5. Also, the boson pair occupancy  $D_B$  changes slightly because the boson number density  $n_B$  changes. The boson pair occupancy  $D_B$  approaches to unity as the boson becomes dilute.

#### IV. SUMMARY

In summary, we have performed a quantum Monte Carlo simulation of Bose-Fermi mixture at finite temperature on the three-dimensional optical lattice. The sign problem from the boson hopping term is avoided by taking only the lowest Matsubara mode, which is valid near the critical point or at high temperature. We have analyzed the off-diagonal long-range order of the boson, the particle number densities, and pair occupancies for attractive and repulsive boson-fermion interaction. We found that the region of the Bose-Einstein condensation is extended as the boson-fermion attraction becomes strong. The particle number profiles obtained from the simulations can be understood in terms of the effective chemical potentials and induced fermion-fermion interaction driven by the boson-fermion interaction.

The present exploratory study is a starting point of more expanded simulations with the ingredients including (i) the bare fermion-fermion interaction, (ii) finite size scaling analysis with several different lattice volumes, (iii) continuum limit in the temporal direction, (iv) taking into account the non-zero Matsubara mode for bosons, and (v) mapping of the phase diagram to the fixed number of bosons and fermions. From the physics point of view, there are various interesting future problems to be examined with our approach, e.g. the superfluidity of fermion pairs induced by the density fluctuation of the background bosons with the boson-fermion coupling, and the properties of the boson-fermion mixture in the strongly coupled regime.

### Acknowledgments

The authors thank Takashi Abe and Ryoichi Seki for useful discussions. A. Y. is supported by the Special

Postdoctoral Research Program of RIKEN. T. H. is partially supported by JSPS Grants-in-Aid No.22340052. The lattice QCD simulations were carried out on NEC SX-8R in Osaka University.

- 
- [1] C. J. Pethick and H. Smoth, *Bose-Einstein Condensation in Dilute Gases*, (Cambridge Univ. Press, London, 2008).
  - [2] K. Maeda, G. Baym and T. Hatsuda, Phys. Rev. Lett. **103**, 085301 (2009).
  - [3] K. Gunter, T. Stoferle, H. Moritz, M. Kohl, and T. Esslinger, Phys. Rev. Lett. **96**, 180402 (2006).
  - [4] C. Ospelkaus, S. Ospelkaus, L. Humbert, P. Ernst, K. Sengstock, and K. Bongs, Phys. Rev. Lett. **97**, 120402 (2006).
  - [5] T. Best, S. Will, U. Schneider, L. Hackermuller, D. - S. Luhmann, D. van Oosten, and I. Bloch, Phys. Rev. Lett. **102**, 030408 (2009).
  - [6] S. Sugawa, K. Inaba, S. Taie, R. Yamazaki, M. Yamashita, and Y. Takahashi, Nature Physics **7**, 642 (2011).
  - [7] Y. Takeuchi and H. Mori, Phys. Rev. A **72**, 063617 (2005); J. Phys. Soc. Jpn. **74**, 3391 (2005); Int. J. of Mod. Phys. B **20**, 617 (2006).
  - [8] L. Pollet, M. Troyer, K. van Houcke, and S. M. A. Rombouts, Phys. Rev. Lett. **96**, 190402 (2006).
  - [9] P. Sengupta and L. P. Pryadko, Phys. Rev. B **75**, 132507 (2007).
  - [10] F. Hebert, F. Haudin, L. Pollet, and G. G. Batrouni, Phys. Rev. A **76**, 043619 (2007)
  - [11] L. Pollet, C. Kollath, U. Schollwock, and M. Troyer, Phys. Rev. A **77**, 023608 (2008)
  - [12] C. N. Varney, V. G. Rousseau, and R. T. Scalettar, Phys. Rev. A **77**, 041608 (2008).
  - [13] A. Masaki, S. Tsukada, and H. Mori, J. Phys. Soc. Jpn. **77**, 054301 (2008).
  - [14] L. Pollet, Rep. Prog. Phys. **75**, 094501 (2012).
  - [15] J. E. Hirsch, R. L. Sugar, D. J. Scalapino, and R. Blankenbecler, Phys. Rev. B **26**, 5033 (1982).
  - [16] N. V. Prokofev, B. V. Svistunov, and I. S. Tupitsyn, JETP **87**, 310 (1998).
  - [17] A. W. Sandvik, Phys. Rev. B **59**, 14157 (1999).
  - [18] For a textbook, H. J. Rothe, *Lattice gauge theories: An Introduction*, World Sci. Lect. Notes Phys. **74**, 1 (2005).
  - [19] A. Yamamoto, Proc. Sci. LATTICE2012, 049 (2012), in press [arXiv:1207.0376 [hep-lat]].
  - [20] P. Hasenfratz and F. Karsch, Phys. Lett. B **125**, 308 (1983).
  - [21] J. -W. Chen and D. B. Kaplan, Phys. Rev. Lett. **92**, 257002 (2004).
  - [22] A. M. Ferrenberg and R. H. Swendsen, Phys. Rev. Lett. **61**, 2635 (1988).
  - [23] D. J. Scalapino and R. L. Sugar, Phys. Rev. B **24**, 4295 (1981).
  - [24] S. Duane, A. D. Kennedy, B. J. Pendleton and D. Roweth, Phys. Lett. B **195**, 216 (1987).